# Regular Wave Height Transformation

**Winyu Rattanapitikon**
Department of Civil Engineering, Sirindhorn International Institute of Technology, Thammasat University, Klong Luang, Phathumthani 12121, Thailand.

**Tomoya Shibayama**
Department of Civil Engineering, Yokohama National University, Tokiwadai, Hodogaya-ku, Yokahama 240, Japan.

## Abstract

Regular wave height transformation is computed from the energy flux conservation based on linear wave theory. The energy dissipation rate is assumed to be proportional to the difference between the local mean energy density and stable energy density. The energy dissipation model is calibrated and verified extensively for a variety of wave and bottom conditions, including small scale and large scale experiments. Published experimental data from eleven sources are better explained by the present energy dissipation model than the preceding model of Dally et al. [1].

## 1. Introduction

Waves play an important role in the coastal area. They have a direct impact on sediment transport and forces on coastal structures. It is essential to have accurate information on wave conditions in the coastal area. As waves propagate shoreward, wave heights increase and eventually break. Once the waves start to break, energy flux from offshore is dissipated to turbulence and heat and causes a decrease in wave height towards the shore in the surf zone.

In the present study, wave height transformation will be computed from the energy flux conservation. It is

$$\frac{\partial(Ec_g)}{\partial x} = -D_B \qquad (1)$$

where $E$ is the wave energy density, $c_g$ is the group velocity, $x$ is the distance in cross shore direction, and $D_B$ is the energy dissipation rate which is zero outside the surf zone.

The main difficulty of energy flux conservation approach is how to compute the energy dissipation rate, $D_B$, inside the surf zone. During the last few decades, a number of studies and experiments have been carried out to develop energy dissipation models. Owing to the complexity of the wave breaking mechanism, any type of model for computing the rate of energy dissipation has to be based on empirical formula calibrated with experimental results. To make the empirical formula reliable, it is necessary to calibrate or verify that formula with a large number and wide range of experimental results. Since many energy dissipation models were developed based on data with limited experimental conditions, there is still a need for more data to confirm the underlying assumptions and to make the model more reliable.

At this moment, the experimental results obtained by many researchers have been accumulated and a large number of experimental results have become available. It is a good time to develop a model based on the large number and wide range of experimental results.

It is the main purpose of this study to develop an energy dissipation model based on a wide range of experimental conditions. Experimental data from 11 sources, including 490 cases, have been collected for calibration and verification of the present energy dissipation models. A summary of the collected experimental results is given in Table 1. The experiments cover a wide range of wave and bottom topography conditions including both small scale and large scale experiments.

**Table 1.** Summary of collected experimental data used to validate the energy dissipation model.

| No | Sources | Total No. of cases | Bed condition | Apparatus |
|---|---|---|---|---|
| 1 | Hansen and Svendsen [2] | 1 | plane beach | small-scale |
| 2 | Horikawa and Kuo [3] | 213 | plane and stepped beach | small-scale |
| 3 | Kajima et al. [4] | 79 | sandy beach | large-scale |
| 4 | Kraus and Smith [5] | 57 | sandy beach | large-scale |
| 5 | Nadaoka et al. [6] | 2 | plane beach | small-scale |
| 6 | Nagayama [7] | 12 | plane, stepped, barred beach | small-scale |
| 7 | Okayasu et al. [8] | 10 | plane beach | small-scale |
| 8 | Sato et al. [9] | 3 | plane beach | small-scale |
| 9 | Sato et al. [10] | 2 | plane beach | small-scale |
| 10 | Shibayama and Horikawa [11] | 10 | sandy beach | small-scale |
| 11 | Smith and Kraus [12] | 101 | plane and barred beach | small-scale |
| | Total | 490 | | |

## 2. Energy Dissipation Model

A major problem of wave field calculation inside the surf zone is how to evaluate the rate of energy dissipation. A number of works on theoretical and experiment studies have been performed to draw a clearer picture of the energy dissipation rate, $D_B$. Various models have been suggested, by previous researchers, for computing the energy dissipation rate, e.g.,

(a) Bore model, originally introduced by Le Mehaute [13], was developed based on an assumption that the energy dissipation rate of a broken wave is similar to the dissipation rate of a hydraulic jump. Several researchers have proposed slightly different forms of the energy dissipation rate, e.g.,

Battjes and Janssen [14]:

$$D_B = \frac{\rho g H^2}{4T} = \frac{2}{T} E \tag{2}$$

Thornton and Guza [15]:

$$D_B = \frac{\rho g H^3}{4Th} = \frac{2H}{Th} E \tag{3}$$

where $\rho$ is the density of water, $g$ is the acceleration due to gravity, $H$ is the wave height, $T$ is the wave period, and $h$ is the water depth.

b) The model of Dally et al. [1], hereafter referred to as Dally model, was developed based on the observation of stable wave height on a horizontal bed. They assumed that the energy dissipation rate is proportional to the difference between the local energy flux and the stable energy flux, divided by the local water depth as

$$D_B \propto \frac{\left[Ec_g - E_s c_g\right]}{h} \tag{4}$$

$$\text{or} \quad D_B = \frac{K_d c_g}{h}\left[E - E_s\right] = \frac{K_d cn}{h}\left[E - E_s\right] \tag{5}$$

where

$$E_s = \frac{1}{8}\rho g H_s^2 = \frac{1}{8}\rho g(\Gamma h)^2 \tag{6}$$

$$n = \left[1 + 2kh/\sinh(2kh)\right]/2 \tag{7}$$

in which $K_d$ is the proportional constant (decay coefficient), $c$ is the phase velocity, $E_s$ is the stable energy density, $H_s$ is the stable wave height, and $\Gamma$ is the stable wave factor.

From the model calibration using the experimental data of Horikawa and Kuo [3], Dally et al. [1] found that $K_d$=0.15 and $\Gamma$ varied case by case between 0.35-0.48. However, finally, they suggested using $\Gamma$=0.4 for general cases. The Dally model has been verified extensively for a variety of wave conditions (e.g., [16], and [17]). The advantage of Dally model is that it is able to reproduce the pause (or stop breaking) in the wave breaking process at a finite wave height on a horizontal bed or in the recovery zone while the bore model gives a continuous dissipation due to wave breaking.

From the above empirical formulas (Eqs. 2-4), we see that the energy dissipation rate, $D_B$, may be a function of the energy density, $E$.

Moreover, the energy dissipation rate, $D_B$, should be equal to zero for recover wave. Therefore, in the present study, the energy dissipation rate, $D_B$, is assumed to be proportional to the difference between the local energy density and stable energy density:

$$D_B \propto [E - E_s] \quad (8)$$

or

$$D_B = \beta [E - E_s] \quad (9)$$

where $\beta$ is the proportionality constant.

Rewriting Eq. (9) in term of wave height:

$$D_B = \beta \frac{\rho g}{8} \left[H^2 - (\Gamma h)^2\right] \quad (10)$$

The energy dissipation rate from Eq. (10) contains two parameters $\beta$ and $\Gamma$ which can be determined empirically from the measured wave heights. The published data from small-scale and large-scale experiments performed under regular wave actions are used to determine the parameters $\beta$ and $\Gamma$. Total 11 sources of published experimental results, including 490 cases, are used in this section (see Table 1).

### 2.1 Determination of the Parameter $\beta$

By comparison of Eq. (9) to Eqs. (2), (3) and (5), respectively, we see that there may be four possible forms of $\beta$. Therefore, there are four possible models of the energy dissipation rate:

model (i):

$$D_B = K_1 \frac{2}{T}(E - E_s) = K_1 \frac{\rho g}{4T}\left[H^2 - (\Gamma h)^2\right] \quad (11)$$

model (ii):

$$D_B = K_2 \frac{2H}{Th}(E - E_s) = K_2 \frac{\rho g H}{4Th}\left[H^2 - (\Gamma h)^2\right] \quad (12)$$

model (iii):

$$D_B = K_3 \frac{cn}{h}(E - E_s) = K_3 \frac{\rho g cn}{8h}\left[H^2 - (\Gamma h)^2\right] \quad (13)$$

model (iv):

$$D_B = K_4 \frac{c}{h}(E - E_s) = K_4 \frac{\rho g c}{8h}\left[H^2 - (\Gamma h)^2\right] \quad (14)$$

where $K_1 - K_4$ are constants, which can be found from model calibrations. It should be noted that; model (iii) (Eq. 13) is the model of Dally et al. [1].

In order to select the proper form of $\beta$ or $D_B$, the above four models (Eqs. 11-14) will be verified against measured wave heights inside the surf zone.

Rewriting Eq. (1) in term of wave height, it becomes

$$\frac{\rho g}{8}\frac{\partial\left(H^2 c_g\right)}{\partial x} = -D_B \quad (15)$$

The wave height transformation is computed from the energy flux balance equation (Eq. 15) by substituting the above possible models of $D_B$ and numerical integrating from breaking point to shoreline. In this subsection, $\Gamma$=0.4 is used as suggested by Dally et al. [1] and it will be modified later in section 2.2.

In order to evaluate the accuracy of the prediction, the verification results are presented in term of root mean square ( *rms* ) relative error, $ER$, as used by Dally et al. [1];

$$ER = 100\sqrt{\sum_{i=1}^{tn}\left(H_{ci} - H_{mi}\right)^2 \Big/ \sum_{i=1}^{tn} H_{mi}^{\,2}} \quad (16)$$

where $i$ is the wave height number, $H_{ci}$ is the computed wave height of number $i$, $H_{mi}$ is the measured wave height of number $i$, and $tn$ is the total number of measured wave height. Smaller values of $ER$ correspond to a better prediction.

A calibration for models (i)-(iv) are conducted by varying the values of $K_1 - K_4$ until the minimize error ($ER$) between measured and computed wave height occur. After the calibration, the optimum values of $K_1 - K_4$ are found to be 0.90, 0.98, 0.15 and 0.15, respectively. The *rms* relative error ($ER$) of each model for all cases of the collected experiments are shown in Table 2.

**Table 2**. Root mean square relative error ( $ER$ ) of the four possible models of $D_B$.

| No | Sources | Total No of cases | $D_B$ from Eq.11 $K_1$=0.90 | $D_B$ from Eq.12 $K_2$=0.98 | $D_B$ from Eq.13 $K_3$=0.15 | $D_B$ from Eq.14 $K_4$=0.15 |
|---|---|---|---|---|---|---|
| 1 | Hansen and Svendsen [2] | 1 | 5.14 | 4.82 | 13.83 | 16.15 |
| 2 | Horikawa and Kuo, slope=0 [3] | 101 | 11.98 | 14.21 | 13.87 | 13.30 |
| | Horikawa and Kuo, slope=1/80-1/20 [3] | 112 | 29.44 | 22.99 | 17.86 | 20.64 |
| 3 | Kajima et al. [4] | 79 | 26.03 | 19.29 | 20.06 | 18.36 |
| 4 | Kraus and Smith [5] | 57 | 21.58 | 26.25 | 21.87 | 20.86 |
| 5 | Nadaoka et al. [6] | 2 | 21.70 | 15.44 | 8.38 | 11.97 |
| 6 | Nagayama [7] | 12 | 10.00 | 9.69 | 9.55 | 9.19 |
| 7 | Okayasu et al. [8] | 10 | 17.39 | 16.06 | 13.57 | 14.18 |
| 8 | Sato et al. [9] | 3 | 15.20 | 12.43 | 8.11 | 11.35 |
| 9 | Sato et al. [10] | 2 | 25.39 | 17.75 | 24.76 | 31.83 |
| 10 | Shibayama and Horikawa [11] | 10 | 19.25 | 17.68 | 17.15 | 16.23 |
| 11 | Smith and Kraus [12] | 101 | 24.73 | 25.11 | 21.98 | 19.44 |
| | Average | | 20.23 | 18.66 | 17.84 | 17.55 |

From Table 2, we see that. the average *rms* relative error of each model is equal to 20.23, 18.66, 17.84 and 17.55, respectively. Therefore, among the four possible models, the model (iv) (Eq. 14) appeared to be the best. Consequently, the proper form of the parameter $\beta$ should be

$$\beta = 0.15\frac{c}{h} \tag{17}$$

Therefore, the energy dissipation rate can be written as

$$D_B = 0.15\frac{c}{h}\left[E - E_s\right]$$
$$= 0.15\frac{c\rho g}{8h}\left[H^2 - (\Gamma h)^2\right] \tag{18}$$

Comparing Eq. (18) with Dally model (Eq. 5), we see that Eq. (18) is similar to the Dally model (Eq. 5) except the factor $n$. The error $ER$ of Eq. (5) is greater than that of Eq. (18). This means that the factor $n$ is not the significant variable. The accuracy of the energy dissipation model will not be improved if we include the factor $n$ in the equation.

### 2.2 Determination of the Parameter $\Gamma$

Since the parameter $\Gamma$ varies between 0.35-0.48 [1], the objective of this subsection is to determine the empirical formula of the parameter $\Gamma$ using the previous experimental results.

After substituting Eq. (18) into Eq. (1), the energy flux balance equation can be written as

$$\frac{\partial(Ec_g)}{\partial x} = 0.15\frac{c\rho g}{8h}\left[H^2 - (\Gamma h)^2\right] \tag{19}$$

Considering Eq. (19), the measured $\Gamma$ can be determined from the measured wave height, period and water depth by using the following formula (rewriting Eq. 19).

$$\Gamma = \frac{1}{h}\sqrt{H^2 - \frac{\partial(Ec_g)}{\partial x}\frac{8h}{0.15c\rho g}} \tag{20}$$

Using the measured wave heights, periods, and water depths from the experimental data of Kajima et al., [4], the measured $\Gamma$ can be determined from Eq. (20). An attempt is made to correlate the parameter $\Gamma$ with the wave parameters. Among the various possibilities, the correlation between $\Gamma$ and $h/\sqrt{LH}$ appeared to be the best (see Fig. 1). A formula for the stable wave factor $\Gamma$, from Fig. 1, can be expressed as

$$\Gamma = \exp\left[-0.36 - 1.25\frac{h}{\sqrt{LH}}\right] \tag{21}$$

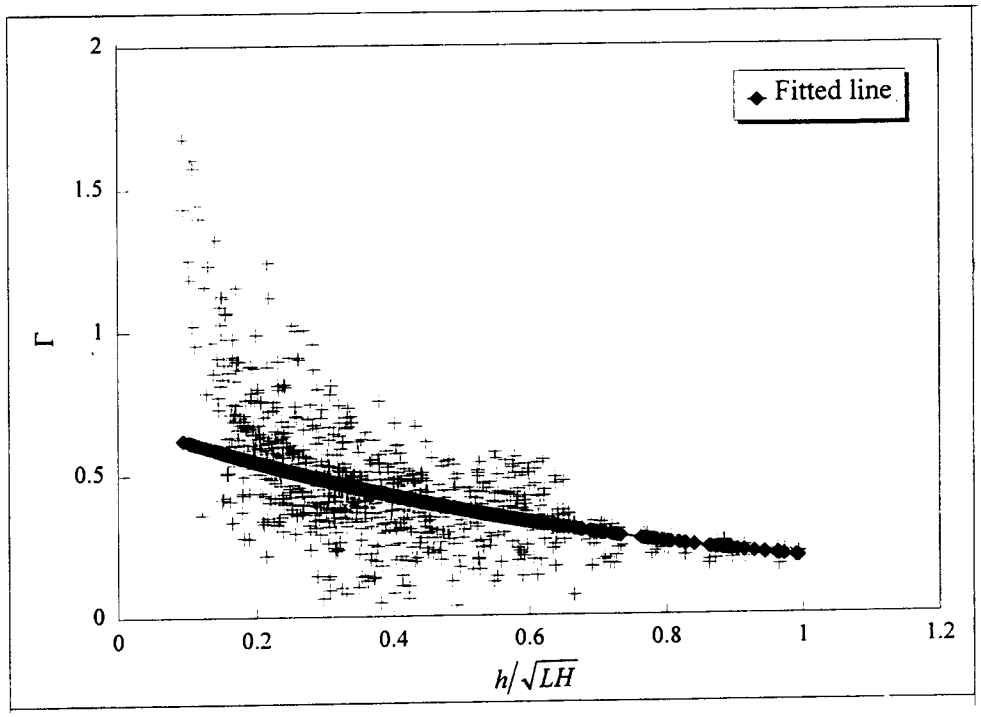


**Figure 1:** Relation between stable wave factor, $\Gamma$, and $h/\sqrt{L/H}$ (laboratory data from Kajima et al., 1983).

Substituting $\Gamma$ from Eq. (21) into Eq. (18), finally, the energy dissipation rate $D_B$ of the present study can be expressed as

$$D_B = \frac{0.15c\rho g}{8h}\left[H^2 - \left(h\exp(-0.36 - \frac{1.25h}{\sqrt{LH}})\right)^2\right] \quad (22)$$

### 2.3 Verification of Energy Dissipation Model

Comparisons between measured and computed wave heights inside the surf zone are used to verify the model. The verification is performed for 490 cases of 11 sources of collected experimental data.

The wave height transformation is computed from the energy flux balance equation (Eq. 1) by substituting $D_B$ from Eq. (22) and numerical integration, using backward finite difference scheme, from breaking point to shoreline. All coefficients in the model are kept to be constant for all cases in the verification.

Table 3 presents results of verification in term of *rms* relative error, *ER*, of each data sources. Column 4 and 5 of Table 3 shows the *rms* relative error, *ER*, of the Dally model (Eq. 5) and the present model (Eq. 22), respectively. From Table 3, we see that the results of computed wave heights inside the surf zone of the present model are better than that of Dally model, for most cases. The average *rms* relative error, *ER*, for all 490 cases of the present model is 15.75 % while that of Dally model is 17.84 %.

## 3. Breaking Location

When waves propagate to the nearshore zone, wave profiles steepen and eventually the waves break and this induces strong turbulence. At the present, the knowledge of breaking waves is not enough to describe details of the breaking process. Empirical methods must be used to a predict the breaking location.

After considering a wide range of data, Goda [18] proposed an empirical breaking index diagram of breaking wave height to depth ratio, as a function of relative water depth for various bottom slopes. However if this diagram is used

**Table 3**. Root mean square relative error ( $ER$ ) of Dally model and present model.

| No | Sources | Total No. of cases | Dally model (Eq.5) | Present study (Eq.22) |
|---|---|---|---|---|
| 1 | Hansen and Svendsen [2] | 1 | 13.83 | 7.00 |
| 2 | Horikawa and Kuo [3], slope=0 | 101 | 13.87 | 11.66 |
| | Horikawa and Kuo [3], slope=1/80-1/20 | 112 | 17.86 | 17.68 |
| 3 | Kajima et al. [4] | 79 | 20.06 | 16.37 |
| 4 | Kraus and Smith [5] | 57 | 21.87 | 19.16 |
| 5 | Nadaoka et al. [6] | 2 | 8.38 | 10.81 |
| 6 | Nagayama [7] | 12 | 9.55 | 8.61 |
| 7 | Okayasu et al. [8] | 10 | 13.57 | 11.26 |
| 8 | Sato et al. [9] | 3 | 8.11 | 7.74 |
| 9 | Sato et al. [10] | 2 | 24.76 | 19.78 |
| 10 | Shibayama and Horikawa [11] | 10 | 17.15 | 17.69 |
| 11 | Smith and Kraus [12] | 101 | 21.98 | 20.44 |
| | Average | | 17.84 | 15.75 |

together with linear wave theory, the predicted breaking point, in some cases, will shift shoreward of the real one. In those cases, linear wave theory gives an under-estimation of wave height just before the breaking point. To avoid this problem, Watanabe et al. [19] used linear wave theory to convert breaking depth diagram of Goda [18] to a diagram of particle velocity-celerity ratio ( $\hat{u}/c$ ) and used it to determine the breaking point [20]. For the convenience of numerical calculation, the diagram of Watanabe et al. [19] was approximated by Isobe [20] as

$$\left(\frac{\hat{u}}{c}\right)_b = 0.53 - 0.3\exp\left[-3\sqrt{\frac{h_b}{L_o}}\right] + 5m_b^{3/2}\exp\left[-45\left(\sqrt{\frac{h_b}{L_o}} - 0.1\right)^2\right] \quad (23)$$

where $\hat{u}$ is the amplitude of horizontal water particle velocity at the mean water level, $L_o$ is the deep-water wavelength, $m_b$ is the bottom slope and subscript $b$ denotes the quantity at breaking point. The variables $\hat{u}$ and $c$ are calculated based on linear wave theory.

Since wave height is the convenient variable in this study, Eq. (23) is transformed in terms of breaking wave height, by using linear wave theory.

$$H_b = \frac{L_o}{\pi \coth^2(k_b h_b)}\left\{0.53 - 0.3\exp\left[-3\sqrt{\frac{h_b}{L_o}}\right] + 5m_b^{3/2}\exp\left[-45\left(\sqrt{\frac{h_b}{L_o}} - 0.1\right)^2\right]\right\} \quad (24)$$

Eq. (24) will be used to compute the location of wave breaking. Since Eq. (24) is originated from Goda breaking depth diagram, Eq. (24) will be called Goda breaking index.

## 4. Wave Model Structure and Results

The numerical model is based on the energy flux conservation (Eq. 1). Backward finite difference scheme is used to compute wave height transformation from energy flux conservation equation. The finite difference method replaces the partial differential operator in Eq. (1) with algebraic operations at the grid points as

$$\frac{1}{8}\rho g\frac{\left(H_i^2 c_{gi} - H_{i-1}^2 c_{gi-1}\right)}{\Delta x} = -D_{Bi-1} \quad (25)$$

or $$H_i = \sqrt{\left(H_{i-1}^2 c_{gi-1} - \frac{8\Delta x}{\rho g} D_{Bi-1}\right)\Big/ c_{gi}} \quad (26)$$

where subscript $i$ denotes the quantity at the grid number $i$.

Eq. (26) enables the grid-by-grid explicit computation of the value $H_i$. The numerical

procedure for computing wave height transformation from offshore to shoreline can be summarized as follows.

1. Input the initial water depth ( $h$ ) at each grid, wave period ( $T$ ) and grid distance ( $\Delta x$ ).

2. Input incident wave height at the first grid.

3. Compute group velocity ( $c_g$ ) for each grid (using linear wave theory).

4. Compute the breaking wave height ( $H_{bi-1}$ ) from Goda breaking index (Eq. 24).

5. If $H_{i-1} < H_{bi-1}$, the wave is in the offshore zone. The wave height can be computed from Eq. (26) by using $D_{Bi-1} = 0$.

6. If $H_{i-1} \geq H_{bi-1}$, the wave is in the surf zone. The wave height can be computed from Eq. (26) by using $D_{Bi-1}$ from Eq. (22).

7. The wave model allows wave reformation to take place when the local wave height reaches the stable wave height in which energy dissipation is equal to zero. In the reformation zone, wave propagates in the same manner as in offshore zone and steps 4-6 will be repeated.

8. The steps 1-7 are repeated until the wave height for all grids have been computed.

9. Mean water level (wave set-up or set-down), $\bar{\varsigma}$, is computed from the momentum conservation equation as

$$\frac{\partial \bar{\varsigma}}{\partial x} = -\frac{1}{\rho g h}\frac{\partial S_{xx}}{\partial x} \tag{27}$$

where $S_{xx} = \left(\frac{1}{2} + \frac{2kh}{\sinh 2kh}\right)E$ is the normal radiation stress in $x$-direction. Backward finite difference scheme is used to solve Eq. (27). The finite difference form of Eq. (27) is expressed as

$$\frac{(\bar{\varsigma}_i - \bar{\varsigma}_{i-1})}{\Delta x} = -\frac{1}{\rho g h}\frac{(S_{xxi} - S_{xxi-1})}{\Delta x} \tag{28}$$

At the offshore boundary, the mean water level is set to be equal to zero. The mean water level, $\bar{\varsigma}$, for all grids can be computed from Eq. (28).

10. The steps 1-9 are repeated until the values of mean water level reach a steady solution. About 2 or 3 iterations are enough to get a steady solution.

Comparisons between measured and computed wave height for all cases of Kajima et al. [4] are shown in Fig. 2. Figs. 3 and 4 show the typical examples of computed and measured wave height transformation. The results of the present wave model can be summarized as follows.

a) In the offshore zone: the computed results show that linear wave theory gives an under estimation of wave height at the location of high Ursell number (near breaking point of case 2.2 in Fig. 3).

b) At the breaking point: case 2.2 of Fig. 3 clearly shows the under estimation of wave height but breaking location, computed from Eq. (24), is quite good. Wave breaking always occurs at the shoreward slope of bar. In some cases, the predicted breaking location shifts seaward of the measured one (e.g., cases 2.1 and 6.1) and some cases are shifted shoreward (e.g., case 2.3). However, Eq. (24) tends to give a good prediction in general cases.

c) In the surf zone: as seen in Figs. 3 and 4, the energy dissipation model gives a good prediction compared with the measured wave height. However, wave reformation in cases 4.2 and 4.3 can not be predicted. Even if we use the value $\Gamma = 0.4$, it still can not predict the wave reformation. This problem is also found by Larson and Kraus [17].

d) In general, we can say that the model gives a reasonably good estimation. The main merit of this model is that it requires only a few seconds to get the solution.

## 5. Conclusions

The energy dissipation model is developed based on a large amount of published experimental results. The form of present energy dissipation model is similar to the model of Dally et al. [1]. The main differences between the present model and Dally model are the factor $n$ and the parameter $\Gamma$. It is found that the factor $n$ is not the significant variable. Therefore factor $n$ is not included in the present model. The main improvement of the present model, compared with Dally model, is caused by the parameter $\Gamma$. The validity of the model is confirmed by small scale and large scale experiments inside the surf zone. The average *rms* relative error, $ER$, of the present energy dissipation model is 15.75 %.

For the wave model: the wave height transformation from offshore to shoreline is computed from the energy flux conservation.

Goda's breaking index (Eq. 24) is used to compute the breaking location. The present energy dissipation model (Eq. 22) is used to compute the energy dissipation rate due to wave breaking. Compared with the experimental data of Kajima et al. [4], the present wave model gives a reasonably good estimation of wave height transformation inside and outside the surf zone.

## Acknowledgments

This research was sponsored by the Thailand Research Fund.

## References

[1] Dally, W.R. Dean, R.G. and Dalrymple, R.A. (1985), Wave Height Variation Across Beach of Arbitrary Profile, J. of Geo. Res., Vol. 90, No. C6, pp. 11917-11927.

[2] Hansen, J.B. and Svendsen, I.A. (1984), A Theoretical and Experiment Study of Undertow, Proc. 19th Coastal Eng. Conf., ASCE, pp. 2246-2262.

[3] Horikawa, K. and Kuo, C.T. (1966), A Study of Wave Transformation Inside Surf Zone, Proc. 10th Coastal Eng. Conf., ASCE, pp. 217-233.

[4] Kajima, R. Shimizu, T. Maruyama, K. and Saito, S. (1983), On-offshore Sediment Transport Experiment by Using large Scale Wave Flume, Collected Data No. 1-8, Central Research Institute of Electric Power Industry, Japan (in Japanese).

[5] Kraus, N.C. and Smith, J.M. (1994), SUPERTANK Laboratory Data Collection Project, Technical Report CERC-94-3, U.S. Army Corps of Engineers, Waterways Experiment Station, Vol. 1-2.

[6] Nadaoka, K. Kondoh, T. and Tanaka, N. (1982), The Structure of Velocity Field Within the Surf Zone Revealed by Means of Laser-Doppler Anemometry, Report of The Port and Harbor Research Institute, Vol. 21, No. 2, pp. 50-102 (in Japanese).

[7] Nagayama, S. (1983), Study on the Change of Wave Height and Energy in the Surf Zone, Bach. Thesis, Civil Eng., Yokohama National University, Japan.

[8] Okayasu, A. Shibayama, T. and Horikawa, K. (1988), Vertical Variation of Undertow in the Surf Zone, Proc. 21st Coastal Eng. Conf., ASCE, pp. 478-491.

[9] Sato, S. Fukuhama, M. and Horikawa, K. (1988), Measurement of Near-Bottom Velocities in Random Waves on a Constant Slope, Coastal Eng. in Japan, JSCE, Vol. 31, No. 2, pp. 219-229.

[10] Sato, S. Isayama, T. and Shibayama, T. (1989), Long-Wave Component in Near-Bottom Velocity Under Random Waves on a Gentle Slope, Coastal Eng. in Japan, JSCE, Vol. 32, No. 2, pp. 149-159.

[11] Shibayama, T. and Horikawa, K. (1986), Sediment Transport due to Breaking Waves, Proc. of JSCE, No. 357/II-3 (Hydraulic and Sanitary), pp. 1509-1522.

[12] Smith, J.M. and Kraus, N.C. (1990), Laboratory Study on Macro-Features of Wave Breaking Over Bars and Artificial Reefs, Technical Report CERC-90-12, U.S. Army Corps of Eng., Waterways Exp. Station.

[13] Le Mehaute (1962), On Non-Saturated Breakers and the Wave Run-Up, Proc. 8th Coastal Eng. Conf., ASCE, pp. 77-92.

[14] Battjes, J. A. and Janssen, J.P.E.M. (1978), Energy loss and Set-Up due to Breaking of Random Waves, Proc. 16th Coastal Eng. Conf., ASCE, pp. 569-587.

[15] Thornton, E.B. and Guza, R.T. (1983), Transformation of Wave Height Distribution, Geophys. Res., Vol. 88, pp. 5925-5983.

[16] Ebersole, B. A. (1987), Measurement and Prediction of Wave Height Decay in the Surf Zone, Proc. Coastal Hydrodynamics '87, ASCE, pp. 1-16.

[17] Larson, M. and Kraus, N.C. (1989), SBEACH: Numerical Model for Simulating Storm-Induced Beach Change, Technical Report CERC-89-9, U.S. Army Corps of Engineers, Waterways Experiment Station.

[18] Goda, Y. (1970), A Synthesis of Breaking Indices, Trans. Japan Soc. Civil Eng., Vol. 2, Part 2, pp. 227-230.

[19] Watanabe, A. Hara, T. and Horikawa, K. (1984), Study on Breaking Condition for Compound Wave Trains, Coastal Engineering in Japan, JSCE, Vol. 27, pp. 71-82.

[20] Isobe, M. (1987), Parabolic Equation Model for Transformation of Irregular Waves Due to Refraction, Diffraction and Breaking, Coastal Eng. in Japan, JSCE., Vol. 30, pp. 33-47.

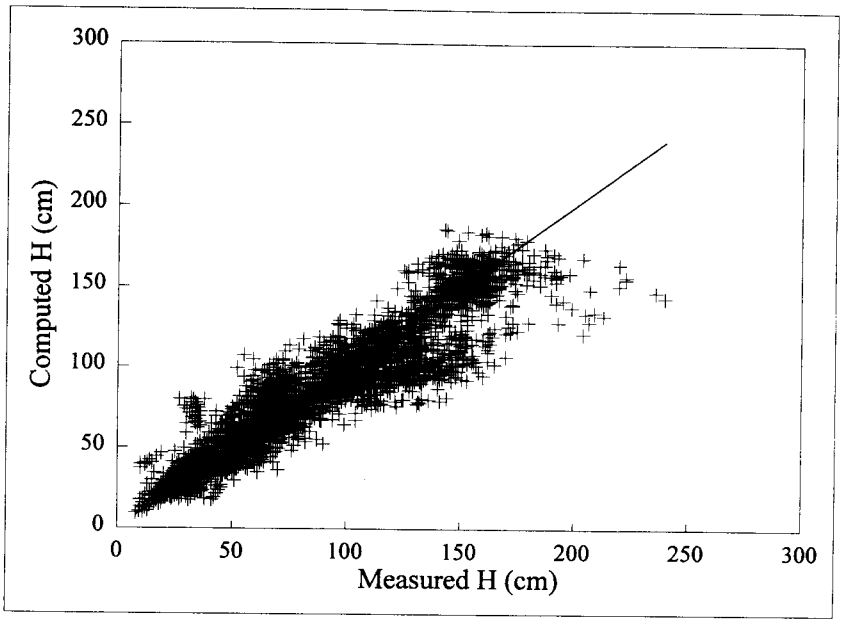


**Figure 2:** Comparison between computed and measured wave heights (measured data from Kajima et al. [4] ).

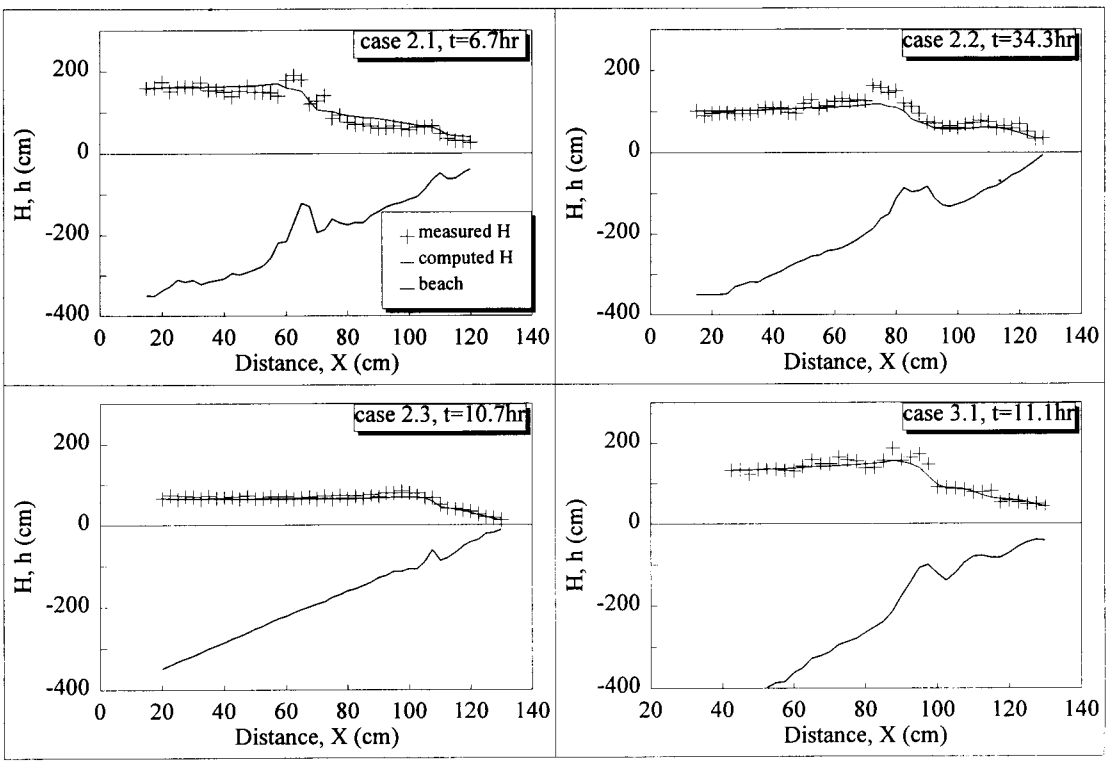


**Figure 3:** Examples of computed and measured wave height transformations (measured data from Kajima et al. [4], cases 2.1, 2.2, 2.3, and 3.1)

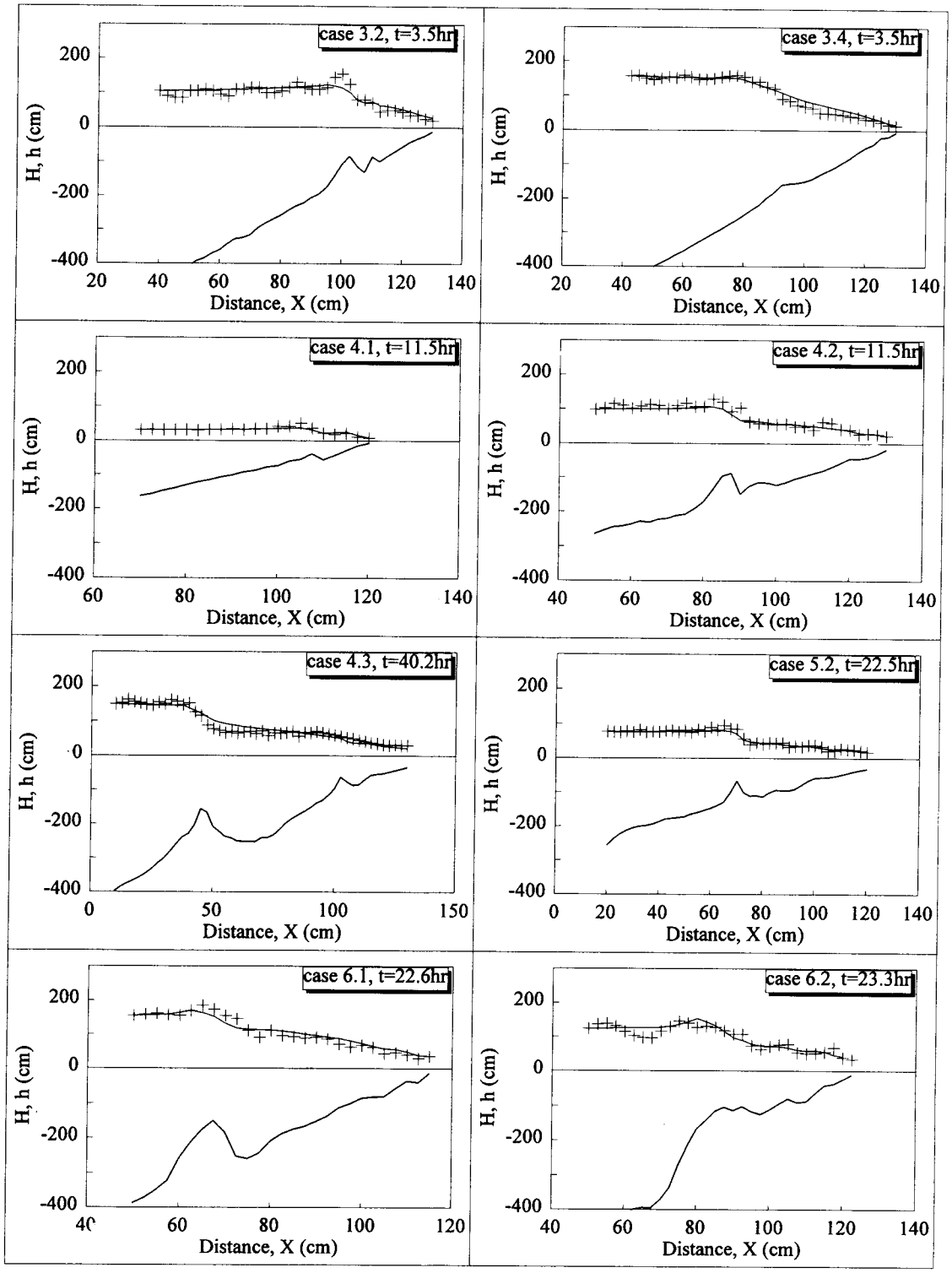


**Figure 4:** Examples of computed and measured wave height transformations (measured data from Kajima et al. [4], cases 3.2, 3.4, 4.1, 4.2, 4.3, 5.2, 6.1, and 6.2).